Available online at www.sciencedirect.com
ScienceDirect
Mendeleev Commun., 2017, **27**, 56–58
Mendeleev Communications

Tetrapod-shaped quantum dots with secondary excitonic luminescence

Aleksandr N. Zolotykh,*[a] Sergey G. Dorofeev,[b] Sergey S. Bubenov[b] and Tatyana A. Kuznetsova[b]

[a] *Department of Materials Science, M. V. Lomonosov Moscow State University, 119991 Moscow, Russian Federation. E-mail: Alekszolotykh@gmail.com*
[b] *Department of Chemistry, M. V. Lomonosov Moscow State University, 119991 Moscow, Russian Federation*

DOI: 10.1016/j.mencom.2017.01.017

The CdSe quantum dots obtained in the presence of chloride ions possess two excitonic bands in luminescence spectra, and one of them can be eliminated by treating the surface of quantum dots in a specific way.

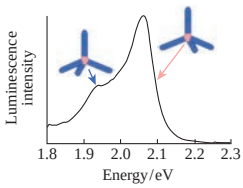

Quantum dots (QDs) have unique optical properties that can be applied to many areas.[1] Different additives induce changes in the morphology and electronic structure of nanocrystals that determine their optical properties. The influence of halide ions on the morphology of QDs was studied extensively.[2–7] Halide anions can cause the epitaxial growth of wurtzite branches on the [111] facets of a zincblende nanocrystal core to cause the formation of a tetrapod structure with unique properties.[8,9]

Double excitonic bands in the emission spectra of QDs were observed,[8,10–12] but the origin of this phenomenon is controversial. Some authors explained it by the inhomogeneity of the sample[12] or by surface traps.[13] Another common approach is to attribute this phenomenon to a wurtzite-sphalerite transition zone in tetrapod-shaped QDs.[14] Type II transition with a long lifetime constant of >100 ns is often observed in this case. According to ref. 15, a double band is caused by exciton recombination both in the core and near the core of tetrapod-shaped QDs. Low energy band originates from charge separation with a lifetime of 62 ns. However, in our work a short lifetime is demonstrated for both bands.

The samples of QDs were obtained by a modified oleate technique.[16,†] All samples obtained in the presence of additives have a branched structure of rods, bipods, tripods and tetrapods (Figure 1). QDs synthesized under the same conditions without chloride ions are characterized by a spherical shape (CdSe sample). The statistical processing of TEM images allowed us to determine the mean diameters and lengths of the branches of tetrapods (Table S1). All tetrapod-shaped samples have a unimodal size distribution (Figure S2). According to XRD data, these nanoparticles have a wurtzite structure (Figure S3), no shift of peak positions was detected with the addition of erbium or cadmium.

An excess of fatty acids in the reaction mixture can affect the morphology of QDs.[17] To eliminate this influence, we synthesized a sample of undoped QDs with the same amount of oleate ions as in Er500. The nanocrystals obtained had a spherical shape (Figure S4), and only one excitonic band was observed in luminescence spectra.

The concentration of erbium was determined relative to the amount of Cd in a sample (Figure 2). The erbium content

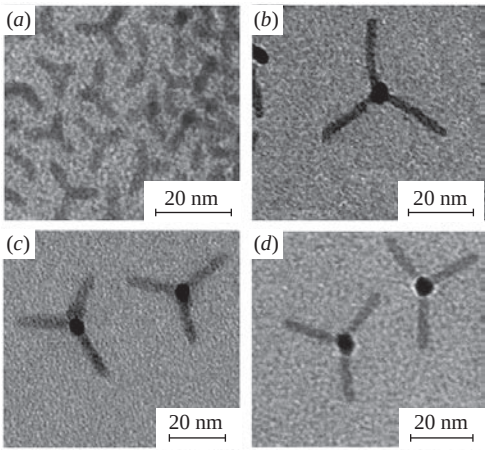

Figure 1 Transition electron microscopy images of quantum dot samples: (*a*) Er100, (*b*) Er300, (*c*) Er500 and (*d*) Cd300.

† *Synthesis of QDs*. Cadmium acetate dihydrate (500 μmol) and oleic acid (1500 μmol) were dissolved in 5 ml of diphenyl ether at 150 °C under argon atmosphere. For different samples variety of precursors were added to the reaction mixture: 300 μmol of $CdCl_2$ or $ZnCl_2$ (samples Cd300 and Zn300); 300 μmol of ytterbium propionate along with 7 wt% of chloride ions (Yb300). The amount of erbium propionate was varied from 20 to 100 mol% relative to Cd (samples Er100–Er500). Erbium propionate was used as is and contained 7 wt% of chloride ions. For the list of all samples, see Table S1 (Online Supplementary Materials). Trioctylphosphine selenide was added to initiate the growing process after heating the mixture to 230 °C, duration of synthesis was 5 min. The mixture was rapidly cooled to room temperature and acetone was added to precipitate QDs out of sol. The precipitate was separated by centrifuging, and then dispersed in hexane. This purification process was repeated 3 times for every sample.

Replacement of stabilizer was performed to purify the surface of QDs from ions adsorbed on the surface and dissolved in the surfactant layer. For this purpose pyridine was added to the solution of QDs in hexane. After removing hexane by air flow, the resulting pyridine sol was left overnight. Then, hexane was added and the solution was centrifuged. The precipitate was redispersed in pyridine. The reverse procedure was carried out to replace pyridine coating with oleate.

A thin layer of QDs was deposited on a glass by drop drying of a sol. Samples were placed in a low pressure (2 Torr) silica tube with atomic H diluted by H_2. Atomic H was generated by capacitively coupled discharge (100 KHz, 50 W) in a separate tube and transported to the sample by the flow of hydrogen.

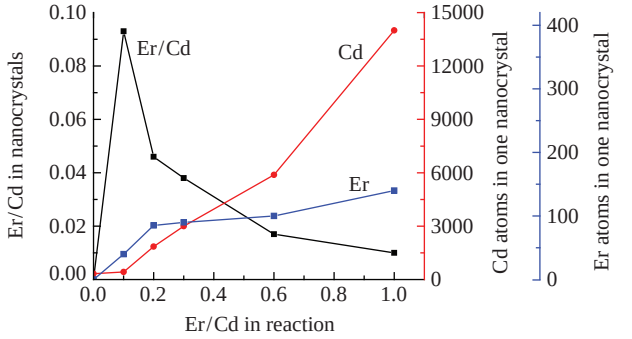

Figure 2 Influence of erbium precursor concentration in reaction mixture on erbium concentration in quantum dots. Mean number of Cd atoms in a quantum dot shown as a reference.

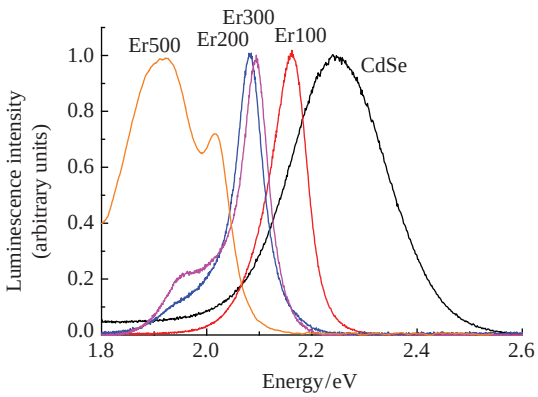

Figure 3 Normalized luminescence spectra of Er-containing samples and undoped CdSe.

normalized to one QD increases with the concentration of erbium propionate in the reaction mixture.

The chemical analysis of the sample Er500 before and after exchanging an oleic acid layer revealed that after changing the stabilizer, the concentration of erbium had dropped significantly (Figure S5). Therefore, erbium ions were on the surface of the QDs, and they were completely removed with the change of the oleic acid layer.

Figure 3 shows the normalized luminescence spectra of erbium doped QDs and a sample of undoped CdSe.

The sample Er100 was characterized by a shift of the luminescence maximum, in comparison to undoped CdSe. This occurs due to the formation of nanoparticles with different morphologies (see TEM images). The second emission band was observed for the sample Er200. This band has energy about 0.2 eV lower than that of the first band. As the amount of erbium was raised further in the series, the second band shifted to lower energies and its intensity increased to exceed the intensity of the first band for the sample Er500. The absorption spectra of these samples are typical of CdSe tetrapod nanoparticles (Figure S6).

Samples with two excitonic bands were prepared in the presence of other dopants such as $ZnCl_2$, $CdCl_2$ and Yb^{3+} with chloride ions in solution (Figure S7). Note that the samples obtained without chloride ions had a spherical shape, and they did not exhibit double excitonic emission (Figure S8).

For the sample Er500, the oleic layer was exchanged to pyridine and back to oleate (Figure 4). As a result, the secondary excitonic band disappeared. We attribute this fact to the removal of erbium ions from the QD surface.

The kinetics of luminescence was measured for two samples (Figure 5). For the sample Er300, luminescence impulses at both wavelengths were identical and coincided with the laser impulse in time. The lifetime was shorter than the detector response time (8 ns). The same applies to the high–energy band (2.1 eV) for the sample Cd300, while the low-energy band (2.0 eV) ceased

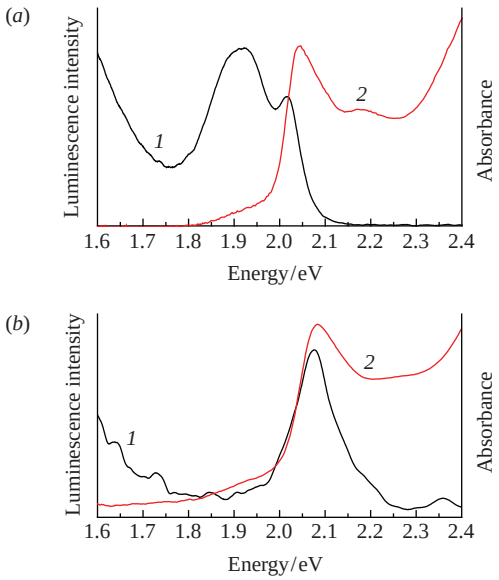

Figure 4 Normalized (*1*) luminescence and (*2*) absorption spectra of the sample Er500 (*a*) before and (*b*) after changing an oleate stabilizer.

earlier than laser impulse; thus, saturation was observed. The band saturation can occur due to the slow relaxation of QDs (lifetime of < 8 ns). Probably, these bands originated from different nanoparticles. For both samples, luminescence lifetimes are < 100 ns; thus, no spatial separation of charges occurs and these luminescence bands are excitonic.[14]

The reduction of the sample Cd300 by atomic hydrogen leads to a decrease of the low-energy emission band (Figure 6). When the sample was left for three days in air, the second band emerged again. This can be explained by the reduction of the oxide layer on the surface of QDs to Cd^0 and the subsequent oxidation of this metallic layer. There are only small changes after the same procedure in the luminescence spectra of erbium samples (Figure S9). This reduction for samples with erbium does not proceed because

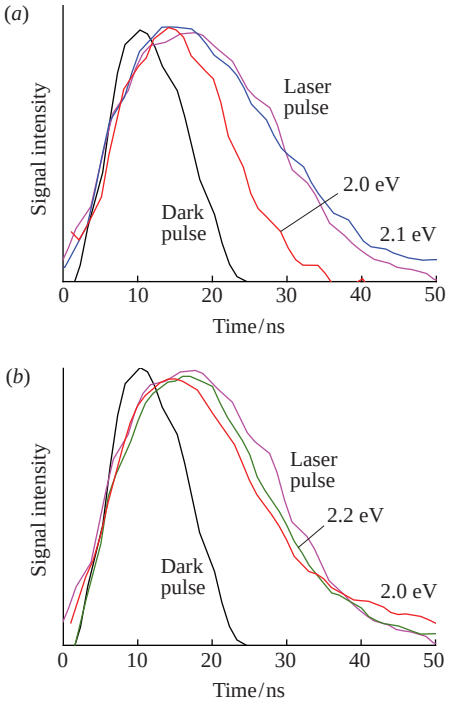

Figure 5 Time dependence of photocurrent impulses at different wavelengths during luminescence for (*a*) Cd300 and (*b*) Er300. Excited and dark impulses are shown as a reference. The dark : luminescence : laser amplitude ratio was 1 : 50 : 250.

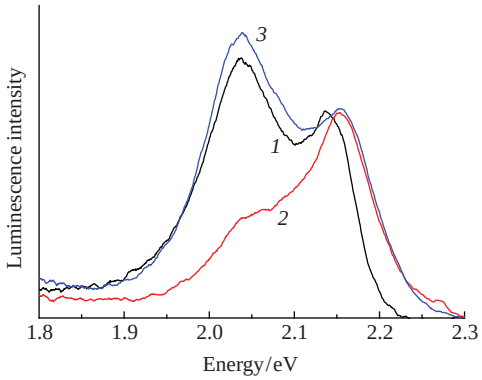

Figure 6 Normalized luminescence spectra of (*1*) initial sample Cd300 and after (*2*) reduction and (*3*) oxidation of the sample.

the Er–O bond is stronger and it cannot be reduced by atomic hydrogen.

We suggest that the second band appears due to the metal-oxide phase on the surface of tetrapod-shaped QDs. Its composition is unknown. It can be MeO_n, $MeO_n(OH)_m$, $Me(OH)_m$, or other phases. The layer originates from the hydrolysis of precursors caused by the presence of a small amount of water in the reaction mixture. The formation of such a layer was demonstrated for spherical QDs, although they did not have double excitonic luminescence.[18] For samples containing erbium assuming that this layer is uniformly distributed on the surfaces of the branches, its thickness should be < 1 nm. This can account for the lack of corresponding peaks appearing on XRD data. Moreover, this layer can be amorphous or insular.

Erbium ion as a hard acid would more likely form oxide rather than selenide and its incorporation in QD lattice seems unlikely. In our case doping does not occur because all erbium ions can be removed by changing the oleate capping.

The difference in the dielectric constants of CdSe (ε = 10.2) and an oxide phase (ε = 12.9 for Er_2O_3 or 21.9 for CdO) can influence the position of exciton in the tetrapod-shaped structure. The Bohr radius of an electron (R_{be} = 3 nm) is greater than the branch radius of tetrapods (r = 1.5–2.0 nm), and the hole radius is smaller (R_{bh} = 1 nm) than this value. Because of that spatial position, the electron and the hole cannot be in the same place, and at a distance of about R_{be} exciton can appear as a charged capacitor. This capacitor tends to pull in the dielectric with higher dielectric constant between the plates. This interaction can lead to exciton placing in the branches of tetrapods where it can recombine with emitting light. That can lead to possible recombination of excitons both in the core (as in usual tetrapods) and in the branches of QDs that occur with different energies and, as a consequence, double bands appear in luminescence spectra.

Thus, a double excitonic band in luminescent spectra is observed for CdSe tetrapods obtained in the presence of the metal and chloride ions in solution. We confirmed that this band originates due to the oxide phase layer on the surface of the branches of tetrapods. Removing the layer by changing the stabilizer or by the reduction of the oxide layer eliminates the secondary band. We suggest that the effect can be due to the different dielectric constants of the oxide layer and tetrapod material that causes radiative exciton recombination in a tetrapod branch.

Online Supplementary Materials

Supplementary data associated with this article can be found in the online version at doi: 10.1016/j.mencom.2017.01.017.

References

1 J. Y. Kim, O. Voznyy, D. Zhitomirsky and E. H. Sargent, *Adv. Mater*., 2013, **25**, 4986.
2 M. R. Kim, K. Miszta, M. Povia, R. Brescia, S. Christodoulou, M. Prato, S. Marras and L. Manna, *ACS Nano*, 2012, **6**, 11088.
3 M. Saruyama, M. Kanehara and T. Teranishi, *J. Am. Chem. Soc*., 2010, **132**, 3280.
4 C. Palencia, K. Lauwaet, L. de la Cueva, M. Acebrón, J. J. Conde, M. Meyns, C. Klinke, J. M. Gallego, R. Otero and B. H. Juárez, *Nanoscale*, 2014, **6**, 6812.
5 M. Lazell and P. O'Brien, *J. Mater. Chem*., 1999, **9**, 1381.
6 M. Meyns, F. Iacono, C. Palencia, J. Geweke, M. D. Coderch, U. E. A. Fittschen, J. M. Gallego, R. Otero, B. H. Juárez and C. Klinke, *Chem. Mater.*, 2014, **26**, 1813.
7 P. A. Kotin, S. S. Bubenov, T. A. Kuznetsova and S. G. Dorofeev, *Mendeleev Commun*., 2015, **25**, 372.
8 Q. Pang, L. Zhao, Y. Cai, D. P. Nguyen, N. Regnault, N. Wang, S. Yang, W. Ge, R. Ferreira, G. Bastard and J. Wang, *Chem. Mater*., 2005, **17**, 5263.
9 J. Lim, W. K. Bae, K. U. Park, L. zur Borg, R. Zentel, S. Lee and K. Char, *Chem. Mater*., 2013, **25**, 1443.
10 N. X. Nghia, L. B. Hai, N. T. Luyen, P. T. Nga, N. T. Thuy Lieu and T.-L. Phan, *J. Phys. Chem. C*, 2012, **116**, 25517.
11 M. De Giorgi, D. Tari, L. Manna, R. Krahne and R. Cingolani, *Microelectron. J*., 2005, **36**, 552.
12 L. Zhao, Q. Pang, S. Yang, W. Ge and J. Wang, *Phys. Lett. A*, 2009, **373**, 2965.
13 J. D. Patel, F. Mighri and A. Ajji, *Mater. Res. Bull.*, 2012, **47**, 2016.
14 G. Morello, A. Fiore, R. Mastria, A. Falqui, A. Genovese, A. Creti, M. Lomascolo, I. R. Franchini, L. Manna, F. D. Sala, R. Cingolani and M. De Giorgi, *J. Phys. Chem. C*, 2011, **115**, 18094.
15 Y. Yang, K. Wu, Z. Chen, B.-S. Jeong and T. Lian, *Chem. Phys*., 2015, **471**, 32.
16 P. N. Tananaev, S. G. Dorofeev, R. B. Vasiliev, K.O. Znamenkov and T. A. Kuznetsova, *Mendeleev Commun*., 2009, **19**, 131.
17 T. Morris and T. Zubkov, *Colloids Surf. A*, 2014, **443**, 439.
18 N. Mordvinova, A. Vinokurov, S. Dorofeev, T. Kuznetsova and K. Znamenkov, *J. Alloys Compd.*, 2014, **582**, 43.

Received: 5th April 2016; Com. 16/4897